

Received June 12, 2018, accepted July 14, 2018, date of publication July 24, 2018, date of current version August 15, 2018.

Digital Object Identifier 10.1109/ACCESS.2018.2859261

# Secrecy Performance Analysis of Artificial-Noise-Aided Spatial Modulation in the Presence of Imperfect CSI

XIANGBIN YU<sup>1,2,3</sup>, (Member, IEEE), YAPING HU<sup>1</sup>, QING PAN<sup>1</sup>,

XIAOYU DANG<sup>1</sup>, (Member, IEEE), NING LI<sup>1</sup>, AND MAQSOOD HUSSAIN SHAN<sup>1</sup>

<sup>1</sup>College of Electronic and Information Engineering, Nanjing University of Aeronautics and Astronautics, Nanjing 210016, China

<sup>2</sup>Key Laboratory of Wireless Sensor Network and Communication, Shanghai Institute of Microsystem and Information Technology, Chinese Academy of Sciences, Shanghai 200050, China

<sup>3</sup>National Mobile Communications Research Laboratory, Southeast University, Nanjing 210096, China

Corresponding author: Xiangbin Yu (yxh-xwy@hotmail.com)

This work was supported in part by the National Natural Science Foundation of China under Grant 61571224 and Grant 61571225, in part by the Open Research Fund Key Laboratory of Wireless Sensor Network and Communication of Chinese Academy of Sciences under Grant 2017006, in part by the Fundamental Research Funds for the Central Universities under Grant 1008-56XZA15009, in part by the Natural Science Foundation of Jiangsu Province in China under Grant SBK2018020206, and in part by the Foundation of Graduate Innovation Center in NUAA under Grant kfjj20170410.

**ABSTRACT** The security of information over wireless channels has always been an important aspect of wireless communication research. In this paper, the secrecy performance of a spatial modulated system with an artificial noise is investigated over the Rayleigh channel, and the corresponding secrecy rate is analyzed in the presence of imperfect channel state information (CSI). Based on the secrecy performance analysis, the ergodic rates and the corresponding lower bounds of the legitimate receiver and eavesdropper are, respectively, derived. As a result, the closed-form lower bound of ergodic rate of the legitimate receiver is obtained, and the lower bound of ergodic rate of the eavesdropper and the corresponding ergodic secrecy rate (ESR) can be achieved by calculating the mean values. To avoid the mean operation and reduce the complexity, the closed-form approximated expression of ESR is also derived. This theoretical ESR can include the one under perfect CSI as a special case and has the value close to the corresponding simulation. Thus, it can provide good performance evaluation for the artificial-noise-aided spatial modulation system with imperfect CSI. Simulation results verify the effectiveness of the theoretical analysis. The system with imperfect CSI is found to have low ESR as compared to the one with perfect CSI due to the estimation error. Moreover, initially, the ESR increases with increasing power of artificial noise, but then, due to the total power constraint, it starts decreasing.

**INDEX TERMS** Artificial noise, ergodic secrecy rate, imperfect channel state information, physical layer security, spatial modulation.

## I. INTRODUCTION

Spatial modulation (SM), has recently received much attention because of its high spectral efficiency and low-complexity capabilities. In SM scheme, only one transmit antenna is usually activated at any time slot and the active antenna indices are used to convey additional information, thereby reducing the inter-channel interference and eliminating the synchronization requirement of transmit antennas [1], [2]. Because of the broadcast nature of wireless signals, the security of transmitted information in SM needs to be improved for against eavesdroppers [3].

Physical layer security is an effective method to enhance the secrecy performance by exploiting the characteristics of

wireless channels [4], [5]. For passive eavesdroppers, they do not transmit any signals but just receive, thus the source does not know any eavesdropper's existence or the channel gain. To solve this problem, artificial noise and other methods such as random subcarrier-selection have been introduced to MIMO systems for secure transmission [6]–[10]. For guaranteeing the secure transmission of SM, some physical layer security schemes for the SM system have been proposed [11]–[13]. Reference [11] provides a precoding scheme for SM with finite alphabet input given that the channel state information (CSI) of source-to-eavesdropper is available at the source. While for the passive eavesdroppers, it is difficult to obtain the prior CSI. To resist

passive eavesdroppers at unknown locations, a low-complexity approach using artificial noise and its corresponding secrecy rate analysis was presented in [12]. For better secrecy performance, a secure unitary coded spatial modulation scheme was proposed in [13], which combined SM with unitary codes for higher diversity at the desired receiver, and it exploited artificial noise to degrade the performance at eavesdropper. Reference [14] considered a full-duplex receiver that simultaneously transmits jamming signals and detects the SM signals. Moreover, an asymptotical approximation of ergodic secrecy rate (ESR) was derived when the number of transmit antennas at the Bob's receiver is very large. All the above mentioned works assume the perfect CSI knowledge for both the main and eavesdropping channel. In practice, however, the influence of imperfect CSI cannot be ignored due to the channel estimation error.

Motivated by the above mentioned reason, we will analyze the secrecy performance of SM system with artificial noise over Rayleigh fading channels for perfect and imperfect CSI, and derive the corresponding approximated expressions of ESR. In this system, the artificial noise is mixed with SM signal to degrade the performance of the eavesdropper. Also, the lower bounds and approximated expressions of ergodic rates at the legitimate receiver and the eavesdropper are, respectively, derived, and subsequently the approximated ESR which contains the mathematical expectation is obtained. To avoid calculating the expectation, an approximated closed-form ESR is further derived. Computer simulation shows that the theoretical results are close to the corresponding simulations under imperfect and perfect CSI, and the secrecy rate becomes lower with the increase of estimation error, which corroborates the validity of the derived expressions.

The notations in this paper are shown as follows. The superscripts  $(\cdot)^T$  and  $(\cdot)^H$  represent the matrix transposition and conjugate transposition, respectively. Bold uppercase letter and bold lowercase letter denote matrix and vector, respectively.  $\mathbb{E}[\cdot]$  stands for the expectation operator and  $\mathbf{0}_{n \times m}$  denotes a  $n \times m$  all-zero matrix.  $\|\cdot\|_F^2$  is the Frobenius norm.

## II. SYSTEM MODEL

In this paper, the secure SM system consists of one source node (Alice), one legitimate receiver (Bob) and one eavesdropper (Eve). Alice is equipped with  $N_a$  transmit antennas, and Bob and Eve are both equipped with single receive antenna. Based on the basic idea of SM, with total  $\log_2(MN_a)$  bits for each transmission,  $\log_2(N_a)$  bits determine the index of active transmit antenna  $i$ ,  $i \in [1, N_a]$ , and  $\log_2 M$  bits are used for  $M$ -ary constellation mapping. Thus the transmitted SM signal is expressed as [15]

$$\mathbf{x}_i = [0 \ 0 \ \cdots \ x_q \ \cdots \ 0]^T \quad (1)$$

where  $x_q$  is the  $i$ -th element and represents the  $q$ -th symbol of  $M$ -ary constellation.

Considering the fact that perfect CSI is hard to obtain in practice due to the estimation errors, we assume that the imperfect CSI of main channel (Alice-to-Bob) is available at

Alice and Eve, and the imperfect CSI of eavesdropping channel (Alice-to-Eve) is available at Eve. The relation between the actual channel  $\mathbf{h}_l$ ,  $l \in [b, e]$  and its estimate can be given by [16]

$$\mathbf{h}_l = \sqrt{1 - \sigma^2} \hat{\mathbf{h}}_l + \sqrt{\sigma^2} \tilde{\mathbf{h}}_l \quad (2)$$

where  $\hat{\mathbf{h}}_{b(e)}$  and  $\tilde{\mathbf{h}}_{b(e)}$  are  $N_a \times 1$  vectors, and represent the estimate and the estimation error of the main (eavesdropping) channel, respectively, and their entries are independent and identically distributed (*i.i.d.*) zero-mean complex Gaussian random variables (*r.v.s*) with unit variance.  $\hat{\mathbf{h}}_b = [\hat{h}_b^1, \hat{h}_b^2, \dots, \hat{h}_b^{N_a}]^T$ ,  $\tilde{\mathbf{h}}_b = [\tilde{h}_b^1, \tilde{h}_b^2, \dots, \tilde{h}_b^{N_a}]^T$ ,  $\hat{\mathbf{h}}_e = [\hat{h}_e^1, \hat{h}_e^2, \dots, \hat{h}_e^{N_a}]^T$  and  $\tilde{\mathbf{h}}_e = [\tilde{h}_e^1, \tilde{h}_e^2, \dots, \tilde{h}_e^{N_a}]^T$ .  $\sigma^2$  is the estimation error variance and reflects the accuracy of the CSI, here, we consider two different models to model  $\sigma^2$ : 1) it is constant independent of SNR; 2) it is a decreasing function of SNR. When  $\sigma^2 = 0$ , perfect CSI is available.

For that the transmitter is only aware of the estimate of  $\hat{\mathbf{h}}_b$ , the null space of  $\hat{\mathbf{h}}_b$  is used to reduce the interference of the artificial noise to Bob. Taking the singular value decomposition of  $\hat{\mathbf{h}}_b$ , we can obtain

$$\hat{\mathbf{h}}_b^T = [d \ \ \mathbf{0}_{1 \times (N_a-1)}] [\mathbf{v}_1 \ \ \mathbf{V}_0]^H \quad (3)$$

where  $d$  is the singular value of  $\hat{\mathbf{h}}_b$  and  $\mathbf{v}_1 \in \mathbb{C}^{N_a \times 1}$  is the singular value vector corresponding to  $d$ .  $\mathbf{V}_0$  is a  $N_a \times (N_a - 1)$  null space of  $\hat{\mathbf{h}}_b$ . Thus, the transmitted signal consisting of SM signal and artificial noise (AN) is expressed as [12], [17]

$$\mathbf{s} = \sqrt{\theta P} \mathbf{x}_i + \sqrt{\frac{(1-\theta)P}{N_a-1}} \mathbf{V}_0 \mathbf{z} \quad (4)$$

where  $P$  is the total transmit power, and  $\theta$  is the coefficient of the power allocated to the SM signal,  $\theta \in [0, 1]$  [18].  $\mathbf{z}$  is a  $(N_a - 1) \times 1$  artificial noise vector whose elements are complex Gaussian distributed with zero mean and unit variance. With this transmitted signal, the received signals at Bob and Eve can be, respectively, given by

$$\begin{aligned} y_b &= \hat{\mathbf{h}}_b^T \mathbf{s} + n_b \\ &= \sqrt{(1-\sigma^2)\theta P} \hat{\mathbf{h}}_b^T \mathbf{x}_i + \sqrt{\frac{(1-\sigma^2)(1-\theta)P}{N_a-1}} \hat{\mathbf{h}}_b^T \mathbf{V}_0 \mathbf{z} \\ &\quad + \sqrt{\sigma^2\theta P} \tilde{\mathbf{h}}_b^T \mathbf{x}_i + \sqrt{\frac{\sigma^2(1-\theta)P}{N_a-1}} \tilde{\mathbf{h}}_b^T \mathbf{V}_0 \mathbf{z} + n_b \\ &= \sqrt{\rho\theta P} \hat{\mathbf{h}}_b^T \mathbf{x}_i \\ &\quad + \underbrace{\sqrt{\sigma^2(1-\theta)P} \tilde{\mathbf{h}}_b^T \mathbf{V}_0 \mathbf{z} + n_b}_{\tilde{n}_b} \end{aligned} \quad (5)$$

and (6) as shown at the top of following page. Where  $\rho = 1 - \sigma^2$ ,  $n_b$  and  $n_e$  are zero-mean complex Gaussian noise with variance of  $N_0$ . The average signal to noise ratio (SNR) is defined as  $\bar{\gamma} = P/N_0$ . Because  $\hat{\mathbf{h}}_b^T \mathbf{V}_0 = \mathbf{0}_{1 \times (N_a-1)}$  and  $\tilde{\mathbf{h}}_b^T \mathbf{V}_0 \neq \mathbf{0}_{1 \times (N_a-1)}$ , the artificial noise is partially eliminated at Bob.

$$y_e = \mathbf{h}_e^T \mathbf{s} + n_e = \sqrt{\rho\theta P} \hat{\mathbf{h}}_e^T \mathbf{x}_i + \underbrace{\sqrt{\frac{\rho(1-\theta)P}{N_a-1}} \hat{\mathbf{h}}_e^T \mathbf{V}_0 \mathbf{z} + \sqrt{\sigma^2\theta P} \tilde{\mathbf{h}}_e^T \mathbf{x}_i + \sqrt{\frac{\sigma^2(1-\theta)P}{N_a-1}} \tilde{\mathbf{h}}_e^T \mathbf{V}_0 \mathbf{z} + n_e}_{\tilde{n}_e} \quad (6)$$

For simplifying the computation and considering that the value of  $\sigma^2$  is generally small,  $\tilde{n}_b$  and  $\tilde{n}_e$  can be approximated as zero-mean complex Gaussian noises with variance  $\eta_b = \sigma^2 P + N_0$  and  $\eta_e = \frac{\rho(1-\theta)P}{N_a-1} \|\hat{\mathbf{h}}_e^T \mathbf{V}_0\|_F^2 + \sigma^2 P + N_0$ , respectively.

After the normalization processing, (5) and (6) can be rewritten as

$$\tilde{y}_b = \sqrt{\frac{\rho\theta P}{\eta_b}} \hat{\mathbf{h}}_b^T \mathbf{x}_i + \hat{n}_b \quad (7)$$

$$\tilde{y}_e = \sqrt{\frac{\rho\theta P}{\eta_e}} \hat{\mathbf{h}}_e^T \mathbf{x}_i + \hat{n}_e \quad (8)$$

where  $\hat{n}_b = \tilde{n}_b / \sqrt{\eta_b}$  and  $\hat{n}_e = \tilde{n}_e / \sqrt{\eta_e}$ .

### III. ERGODIC SECRECY RATE

In this section, the lower-bounds and approximated expressions of ergodic rates at Bob and Eve are derived, respectively. Based on this, two approximated expressions of ESR for the artificial-noise-aided SM system with imperfect CSI are obtained subsequently. The ESR of the system is expressed as [14], [19]

$$R_s = [R_b - R_e]^+ \quad (9)$$

where  $[x]^+$  denotes  $\max\{x, 0\}$ ,  $R_b$  and  $R_e$  are the ergodic rates at Bob and Eve, respectively.

#### A. ERGODIC RATE OF BOB

In this subsection, we will derive the ergodic rate of Bob. With (7), the probability density function (PDF) of  $\tilde{y}_b$  is given by [12]

$$p(\tilde{y}_b) = \frac{1}{MN_a} \sum_{i=1}^{N_a} \sum_{q=1}^M \frac{1}{\pi} \exp \left( - \left| \tilde{y}_b - \sqrt{\frac{\rho\theta P}{\eta_b}} \hat{h}_b^i x_q \right|^2 \right) \quad (10)$$

Using (10), the ergodic rate at Bob can be expressed as

$$\begin{aligned} R_b &= \mathbb{E}_{\hat{\mathbf{h}}_b} \left[ \int_{\tilde{y}_b} \sum_{i=1}^{N_a} \sum_{q=1}^M p(\tilde{y}_b, x_q, \hat{h}_b^i) \log_2 \frac{p(\tilde{y}_b | x_q, \hat{h}_b^i)}{p(\tilde{y}_b)} d\tilde{y}_b \right] \\ &= \log_2 MN_a - \frac{1}{MN_a} \sum_{i=1}^{N_a} \sum_{q=1}^M \mathbb{E}_{\hat{\mathbf{h}}_b} \left[ \mathbb{E}_{\hat{n}_b} \left[ \log_2 \sum_{j=1}^{N_a} \sum_{m=1}^M \right. \right. \\ &\quad \times \exp \left( - \left( \left| \sqrt{\frac{\rho\theta P}{\eta_b}} d_{b,qm}^{ij} + \hat{n}_b \right|^2 - |\hat{n}_b|^2 \right) \right) \left. \right] \end{aligned} \quad (11)$$

where  $d_{b,qm}^{ij} = \hat{h}_b^i x_q - \hat{h}_b^j x_m$ .

By means of Jensen's inequality, the lower bound of  $R_b$  is obtained as

$$\begin{aligned} R_b^{low} &= \log_2(MN_a) - \frac{1}{MN_a} \sum_{i=1}^{N_a} \sum_{q=1}^M \log_2 \sum_{j=1}^{N_a} \sum_{m=1}^M \\ &\quad \times \mathbb{E}_{\hat{\mathbf{h}}_b} \left[ \mathbb{E}_{\hat{n}_b} \left[ \exp \left( - \left( \left| \sqrt{\frac{\rho\theta P}{\eta_b}} d_{b,qm}^{ij} + \hat{n}_b \right|^2 - |\hat{n}_b|^2 \right) \right) \right] \right] \\ &= \log_2(MN_a) + 1 - \frac{1}{\ln 2} \\ &\quad - \frac{1}{MN_a} \sum_{i=1}^{N_a} \sum_{q=1}^M \log_2 \sum_{j=1}^{N_a} \sum_{m=1}^M \mathbb{E}_{\hat{\mathbf{h}}_b} \left[ \exp \left( - \frac{\rho\theta P |d_{b,qm}^{ij}|^2}{2\eta_b} \right) \right] \\ &= \log_2(MN_a) + 1 - \frac{1}{\ln 2} \\ &\quad - \frac{1}{MN_a} \sum_{i=1}^{N_a} \sum_{q=1}^M \log_2 \sum_{j=1}^{N_a} \sum_{m=1}^M \frac{\eta_b}{\eta_b + \rho\theta P \lambda_{qm}} \end{aligned} \quad (12)$$

where  $\lambda_{qm} = \begin{cases} (|x_q|^2 + |x_m|^2)/2, & i \neq j \\ |x_q - x_m|^2/2, & \text{else} \end{cases}$ . When  $\sigma^2$  is a very small constant or a decreasing function of SNR, we can derive that  $\lim_{\bar{\gamma} \rightarrow 0} R_b = 0$ ,  $\lim_{\bar{\gamma} \rightarrow \infty} R_b = \log_2(MN_a)$ ,  $\lim_{\bar{\gamma} \rightarrow 0} R_b^{low} = 1 - 1/\ln 2$  and  $\lim_{\bar{\gamma} \rightarrow \infty} R_b^{low} = \log_2(MN_a) + 1 - 1/\ln 2$ .  $R_b$  and  $R_b^{low}$  have the same difference of  $\log_2(MN_a)$  between the high and low SNR regions. Moreover,  $R_b$  and  $R_b^{low}$  are monotonically increasing functions of SNR. These results imply that the difference between  $R_b$  and  $R_b^{low}$  is approximately equal to  $(1 - 1/\ln 2)$  for whole SNR range [14]. Thus, we can derive the approximated  $R_b$  as

$$\begin{aligned} R_b^{app} &= \log_2(MN_a) \\ &\quad - \frac{1}{MN_a} \sum_{i=1}^{N_a} \sum_{q=1}^M \log_2 \sum_{j=1}^{N_a} \sum_{m=1}^M \frac{\eta_b}{\eta_b + \rho\theta P \lambda_{qm}} \end{aligned} \quad (13)$$

The lower bound (12) and the corresponding approximation (13) are verified by simulation (which is analyzed in section IV), and it is shown that they both conform to the simulation results.

#### B. ERGODIC RATE OF EVE

In this subsection, we will derive the ergodic rate of Eve. By using the derivation process similar to that of  $R_b$ ,

the ergodic rate of Eve is achieved as

$$R_e = \log_2(MN_a) - \frac{1}{MN_a} \sum_{i=1}^{N_a} \sum_{q=1}^M \mathbb{E}_{\hat{\mathbf{h}}_e} \left[ \mathbb{E}_{\hat{n}_e} \left[ \log_2 \sum_{j=1}^{N_a} \sum_{m=1}^M \right. \right. \\ \times \exp \left( - \left( \left| \sqrt{\frac{\rho\theta P}{\eta_e}} d_{e,qm}^{ij} + \hat{n}_e \right|^2 - |\hat{n}_e|^2 \right) \right) \left. \right] \right] \quad (14)$$

where  $d_{e,qm}^{ij} = \hat{h}_e^i x_q - \hat{h}_e^j x_m$ .

Correspondingly, the lower bound of  $R_e$  can be obtained by the Jensen's inequality as follows:

$$R_e^{low} = \log_2(MN_a) + 1 - \frac{1}{\ln 2} - \frac{1}{MN_a} \sum_{i=1}^{N_a} \sum_{q=1}^M \log_2 \sum_{j=1}^{N_a} \sum_{m=1}^M \\ \times \mathbb{E}_{\hat{\mathbf{h}}_e} \left[ \exp \left( - \frac{\rho\theta P |d_{e,qm}^{ij}|^2}{2 \left( \frac{\rho(1-\theta)P}{N_a-1} \|\hat{\mathbf{h}}_e^T \mathbf{V}_0\|_F^2 + \sigma^2 P + N_0 \right)} \right) \right] \quad (15)$$

To obtain the theoretical result closer to the actual value, a better approximated  $R_e$  is also given by abandoning the term of  $(1 - 1/\ln 2)$ , i.e., it is expressed as

$$R_e^{app} = \log_2(MN_a) - \frac{1}{MN_a} \sum_{i=1}^{N_a} \sum_{q=1}^M \log_2 \sum_{j=1}^{N_a} \sum_{m=1}^M \\ \times \mathbb{E}_{\hat{\mathbf{h}}_e} \left[ \exp \left( - \frac{\rho\theta P |d_{e,qm}^{ij}|^2}{2 \left( \frac{\rho(1-\theta)P}{N_a-1} \|\hat{\mathbf{h}}_e^T \mathbf{V}_0\|_F^2 + \sigma^2 P + N_0 \right)} \right) \right] \quad (16)$$

Considering that equations (15) and (16) need to calculate the mathematical expectations, which will improve the complexity of computation, a simple approximated closed-form expression of  $R_e$  will be derived. Let  $\gamma_1 = \frac{\rho\theta P |d_{e,qm}^{ij}|^2}{2(\sigma^2 P + N_0)}$  and  $\gamma_2 = \frac{\rho(1-\theta)P \|\hat{\mathbf{h}}_e^T \mathbf{V}_0\|_F^2}{N_a-1}$ , then the PDFs of  $\gamma_1$  and  $\gamma_2$  can be, respectively, given by

$$f_{\gamma_1}(\gamma) = \frac{1}{\bar{\gamma}_1} \exp \left( -\frac{\gamma}{\bar{\gamma}_1} \right) \quad (17)$$

$$f_{\gamma_2}(\gamma) = \frac{1}{\Gamma(N_a-1)} \bar{\gamma}_2 \left( \frac{\gamma}{\bar{\gamma}_2} \right)^{N_a-2} \exp \left( -\frac{\gamma}{\bar{\gamma}_2} \right) \quad (18)$$

where  $\bar{\gamma}_1 = \frac{\rho P \lambda_{qm}}{\sigma^2 P + N_0}$ ,  $\bar{\gamma}_2 = \frac{\rho(1-\theta)P}{(N_a-1)(\sigma^2 P + N_0)}$ . Thus, the expectation in (15) and (16) can be calculated as

$$\mathbb{E}_{\hat{\mathbf{h}}_e} \left[ \exp \left( -\frac{\gamma_1}{\gamma_2 + 1} \right) \right] = \mathbb{E}_{\hat{\mathbf{h}}_e} [\exp(-\gamma_0)] \quad (19)$$

where  $\gamma_0 = \frac{\gamma_1}{\gamma_2 + 1}$ . Considering that the elements of  $\mathbf{h}_e^T \mathbf{V}_0$  are the linear combination of  $N_a$  elements of  $\mathbf{h}_e$  based on the null space  $\mathbf{V}_0$ , and  $d_{e,qm}^{ij}$  is the linear combination of two elements of  $\mathbf{h}_e$  based on the constellation symbol  $\{x_q, x_m\}$ , while  $\mathbf{V}_0$  and  $\{x_q, x_m\}$  are quite different and unrelated. According to this, we may neglect the correlation between  $\|\hat{\mathbf{h}}_e^T \mathbf{V}_0\|_F^2$  and  $|d_{e,qm}^{ij}|^2$ , and utilize their PDFs to derive an approximated closed-form expression of the cumulative distribution function (CDF) of  $\gamma_0$ , i.e.,

$$F_{\gamma_0}(\gamma) = \Pr \left( \frac{\gamma_1}{\gamma_2 + 1} \leq \gamma \right) \\ = \int_0^\infty \int_0^{\gamma(\gamma_2+1)} f_{\gamma_1}(\gamma_1) d\gamma_1 f_{\gamma_2}(\gamma_2) d\gamma_2 \\ = 1 - \exp \left( -\frac{\gamma}{\bar{\gamma}_1} \right) \left( 1 + \frac{\bar{\gamma}_2}{\bar{\gamma}_1} \gamma \right)^{-(N_a-1)} \quad (20)$$

With this CDF, (19) can be rewritten as

$$\mathbb{E}_{\hat{\mathbf{h}}_e} [\exp(-\gamma_0)] \\ = 1 - \int_0^\infty \frac{(1 + \bar{\gamma}_2 \gamma_0 / \bar{\gamma}_1)^{-(N_a-1)}}{\exp[(1 + 1/\bar{\gamma}_1) \gamma_0]} d\gamma_0 \\ = 1 - \frac{\bar{\gamma}_1}{\bar{\gamma}_2} \left( \frac{\bar{\gamma}_1 + 1}{\bar{\gamma}_2} \right)^{\frac{N_a-3}{2}} \\ \times \exp \left( \frac{\bar{\gamma}_1 + 1}{2\bar{\gamma}_2} \right) W_{\frac{1-N_a}{2}, \frac{2-N_a}{2}} \left( \frac{\bar{\gamma}_1 + 1}{\bar{\gamma}_2} \right) \quad (21)$$

where  $W_{\lambda,\mu}(z)$  is the Whittaker function [20].

Substituting (21) into (16) yields the approximated closed-form expression of  $R_e$  as

$$R_e^{app\_cf} = \log_2(MN_a) - \frac{1}{MN_a} \sum_{i=1}^{N_a} \sum_{q=1}^M \log_2 \sum_{j=1}^{N_a} \sum_{m=1}^M \\ \times \left[ 1 - \frac{\bar{\gamma}_1}{\bar{\gamma}_2} \left( \frac{\bar{\gamma}_1 + 1}{\bar{\gamma}_2} \right)^{\frac{N_a-3}{2}} \right. \\ \left. \times \exp \left( \frac{\bar{\gamma}_1 + 1}{2\bar{\gamma}_2} \right) W_{\frac{1-N_a}{2}, \frac{2-N_a}{2}} \left( \frac{\bar{\gamma}_1 + 1}{\bar{\gamma}_2} \right) \right] \quad (22)$$

$$R_s^{app} = \left[ R_b^{low} - R_e^{low} \right]^+ \\ = \left[ \frac{1}{MN_a} \sum_{i=1}^{N_a} \sum_{q=1}^M \log_2 \left( \frac{\sum_{j=1}^{N_a} \sum_{m=1}^M \mathbb{E}_{\hat{\mathbf{h}}_e} \left[ \exp \left( - \frac{\rho\theta P |d_{e,qm}^{ij}|^2 / 2}{\frac{\rho(1-\theta)P}{N_a-1} \|\hat{\mathbf{h}}_e^T \mathbf{V}_0\|_F^2 + \sigma^2 P + N_0} \right) \right]}{\sum_{j=1}^{N_a} \sum_{m=1}^M \eta_b / (\eta_b + \rho\theta P \lambda_{qm})} \right]^+ \right] \quad (23)$$

Equation (22) is an approximated closed-form expression of (16) since the correlation between  $\gamma_1$  and  $\gamma_2$  is neglected, but their difference is smaller since the correlation is relatively weak, which will be shown by the simulation results.

Hence, with (9), we can obtain an approximated expression of ESR as follows (23), as shown at the bottom of the previous page: and approximated closed-form expression of ESR as shown at the bottom of the page.

With these expressions, the theoretical ESRs can be calculated which are also corroborated by simulations. Moreover, equation (24) has lower complexity because it does not require computing the mean value. For perfect CSI, the estimation error variance  $\sigma^2 = 0$ ,  $\rho = 1$ ,  $\eta_b = N_0$ , then (23) is reduced to (25), as shown at the bottom of this page and (24), as shown at the bottom of this page can be reduced to (26) as shown at the bottom of next page, where  $\tilde{\gamma}_1 = \frac{\theta P \lambda_{qm}}{N_0}$ ,  $\tilde{\gamma}_2 = \frac{(1-\theta)P}{(N_a-1)N_0}$ .

Equations (25) and (26) are the approximated and closed-form expressions of the ESR in the presence of perfect CSI, respectively. Theoretical results above are found to be in good agreement with simulations, which will be testified by the following simulation.

#### IV. SIMULATION

In this section, the secrecy performance of artificial-noise-aided SM system under Rayleigh channel with imperfect CSI is evaluated by simulations and the derived theoretical expressions, and the impacts of estimation error variance  $\sigma^2$  and power allocation coefficient  $\theta$  are also analyzed. In simulations, the total power is normalized to one, and correspondingly, the noise variance is given by  $N_0 = 1/\bar{\gamma}$ , where  $\bar{\gamma}$  is the average SNR. The number of transmit antennas  $N_a = 4$  and the modulation size is  $M = 16$  (16QAM). We perform Monte Carlo experiments consisting of 10000 independent trials to obtain the average results.

Fig. 1 and Fig. 2 illustrate the ergodic rates of Bob and Eve with  $\theta = 0.5$ , respectively. The estimation error variance  $\sigma^2 = 1/(\tau\bar{\gamma})$ , where  $\tau$  is related to the length of pilot sequence, and we set  $\tau = 10$  in these two figures.

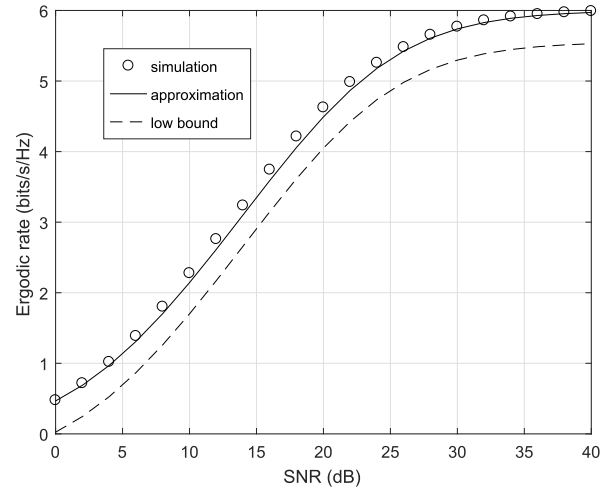


FIGURE 1. Ergodic rate of Bob with imperfect CSI.

In Fig. 1, the lower bound of the ergodic rate at Bob is calculated by (12), and the approximated one is computed by (13). It is found that the approximated ergodic rate is very close to the simulation due to better approximation. Besides, since the approximated ergodic rate is obtained by omitting the term of  $(1 - 1/\ln 2)$  in low bound, the gap between the simulation result and the lower bound is a constant, i.e.,  $(1/\ln 2 - 1)$ . This result shows the effectiveness of (13), and that omitting the term of  $(1 - 1/\ln 2)$  in (12) is also valid, and can make the theoretical value closer to the corresponding simulation. Moreover, from Fig. 1, we can observe that when the average SNR  $\bar{\gamma}$  is large, Bob will obtain the ergodic rate of  $\log_2(MN_a)$ , which accords with the asymptotical analysis below (12).

In Fig. 2, the lower bound and the approximation of the ergodic rate at Eve are, respectively, calculated by (15) and (16), and these expressions include the calculation of expectation. The approximated closed-form ergodic rate is obtained by (22). As Fig. 2 illustrates, the approximated and the approximated closed-form curves nearly have the same values. Moreover, compared with the lower bound, the approximated results are closer to the simulation.

$$R_s^{app\_cf} = \left[ R_b^{app} - R_e^{app\_cf} \right]^+ = \left[ \frac{1}{MN_a} \sum_{i=1}^{N_a} \sum_{q=1}^M \log_2 \left( \frac{\sum_{j=1}^{N_a} \sum_{m=1}^M \left[ 1 - \frac{\tilde{\gamma}_1}{\tilde{\gamma}_2} \left( \frac{\tilde{\gamma}_1+1}{\tilde{\gamma}_2} \right)^{\frac{N_a-3}{2}} \exp\left(\frac{\tilde{\gamma}_1+1}{2\tilde{\gamma}_2}\right) W_{\frac{1-N_a}{2}, \frac{2-N_a}{2}} \left( \frac{\tilde{\gamma}_1+1}{\tilde{\gamma}_2} \right) \right]}{\sum_{j=1}^{N_a} \sum_{m=1}^M \eta_b / (\eta_b + \rho \theta P \lambda_{qm})} \right] \right]^+ \quad (24)$$

$$R_s^{app\_per} = \left[ \frac{1}{MN_a} \sum_{i=1}^{N_a} \sum_{q=1}^M \log_2 \left( \frac{\sum_{j=1}^{N_a} \sum_{m=1}^M \mathbb{E}_{\hat{\mathbf{h}}_e} \left[ \exp \left( - \frac{\theta P |d_{e,qm}^{ij}|^2 / 2}{\frac{(1-\theta)P}{N_a-1} \|\hat{\mathbf{h}}_e^T \mathbf{V}_0\|_F^2 + N_0} \right) \right]}{\sum_{j=1}^{N_a} \sum_{m=1}^M N_0 / (N_0 + \theta P \lambda_{qm})} \right] \right]^+ \quad (25)$$

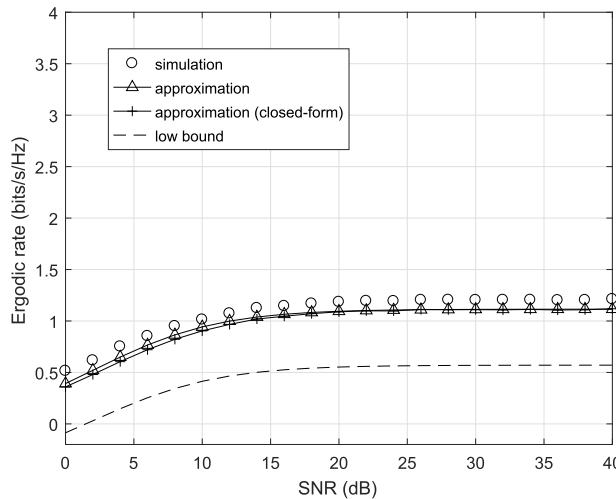


FIGURE 2. Ergodic rate of Eve with imperfect CSI.

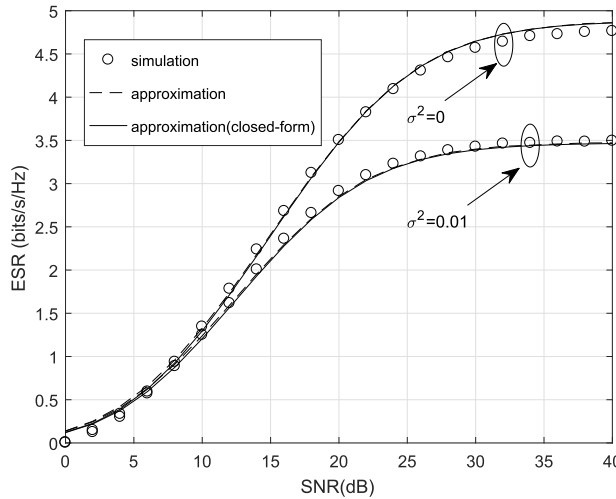
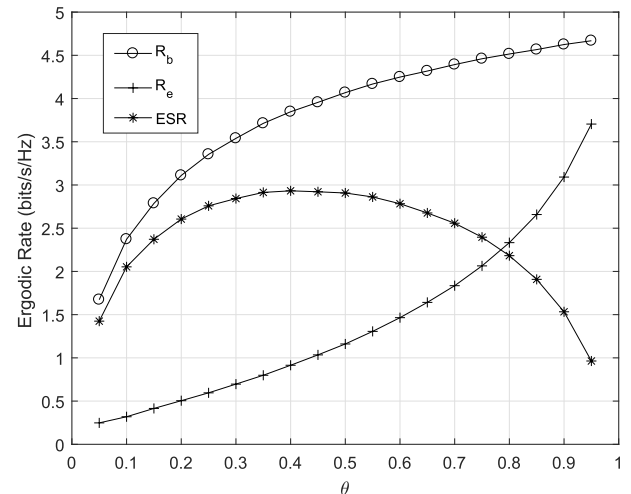


FIGURE 3. ESR of the AN-aided SM systems with perfect CSI and imperfect CSI.

The results above indicate that these theoretical expressions of the ergodic rate at Eve are also valid.

In Figs.3-5, we consider another model of the estimation error, where  $\sigma^2$  is constant. In Fig. 3 shows the theoretical and simulated ESRs of the SM system versus SNR with  $\theta = 0.5$ , where perfect CSI ( $\sigma^2 = 0$ ) and imperfect CSI ( $\sigma^2 = 0.01$ ) are both considered. The approximated and approximated closed-form ESR are obtained by (23), (24) for imperfect CSI and by (25), (26) for perfect CSI, respectively.

FIGURE 4. ESR of the AN-aided SM system versus  $\theta$ .

As seen in Fig. 3, the approximated results agree with the corresponding simulations for both perfect and imperfect CSI, which indicates that these theoretical expressions are also valid for both perfect and imperfect CSI. Comparing the approximated ESR with approximated closed-form ESR, they only have small difference at low SNR, and nearly approach to be consistent at high SNR. The result above indicates that the derived approximated closed-form expression can effectively evaluate the ESR performance of the SM system with low complexity. Furthermore, the ESR under imperfect CSI ( $\sigma^2 = 0.01$ ) is lower than that under perfect CSI ( $\sigma^2 = 0$ ). The reason for the performance degradation is due to the estimation error.

Fig. 4 illustrates the ergodic rates at Bob and Eve as well as the ESR of the system versus power allocation coefficient  $\theta$ , where the SNR is set equal to 20 dB and  $\sigma^2 = 0.01$ . As shown in Fig. 4, the ergodic rates at Bob and Eve both starts to grow with the increase of  $\theta$ . This is because when  $\theta$  increases, the power allocated to SM signal raises and that allocated to artificial noise reduces. The ESR increases when  $\theta$  is smaller than 0.4, and then decrease when  $\theta$  is higher than 0.4. With  $\theta = 0.4$ , the ESR achieved the optimal value. The reason for this is that the ergodic rate at Bob grows faster than that at Eve for low  $\theta$ , and the case for high  $\theta$  is the opposite. As a result, the difference of their ergodic rates, i.e., the ESR, increases at first and then decreases with the increase of  $\theta$ .

Fig. 5 depicts the ergodic rates at Bob and Eve as well as the ESR of the system versus the variance of estimation error  $\sigma^2$ ,

$$R_s^{app\_cf\_per} = \left[ \frac{1}{MN_a} \sum_{i=1}^{N_a} \sum_{q=1}^M \log_2 \left( \frac{\sum_{j=1}^{N_a} \sum_{m=1}^M \left[ 1 - \frac{\tilde{\gamma}_1}{\tilde{\gamma}_2} \left( \frac{\tilde{\gamma}_1+1}{\tilde{\gamma}_2} \right)^{\frac{N_a-3}{2}} \exp \left( \frac{\tilde{\gamma}_1+1}{2\tilde{\gamma}_2} \right) W_{\frac{1-N_a}{2}, \frac{2-N_a}{2}} \left( \frac{\tilde{\gamma}_1+1}{\tilde{\gamma}_2} \right) } \right]}{\sum_{j=1}^{N_a} \sum_{m=1}^M N_0 / (N_0 + \theta P \lambda_{qm})} \right)^+ \right] \quad (26)$$

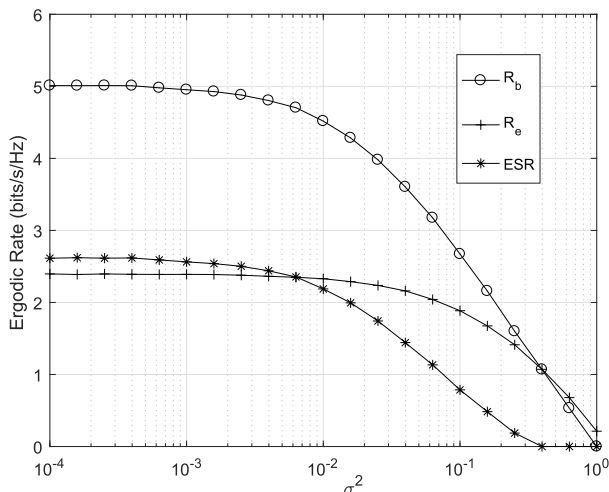


FIGURE 5. ESR of the AN-aided SM system versus  $\sigma^2$ .

where the SNR is equal to 20 dB and  $\theta = 0.8$ . From Fig. 5, it is found that the ergodic rate of Bob and the system ESR can tolerate  $\sigma^2$  up to about 0.001 with a slight degradation, while the ergodic rate of Eve can tolerate the estimation error variance up to about 0.01 with a slight degradation. However, when  $\sigma^2$  increases beyond 0.01, the ESR of the system degrades obviously. Besides, when  $\sigma^2$  decreases to a certain value, the ESR will tend to zero since the ergodic rate at Bob becomes lower than that at Eve under this case.

## V. CONCLUSION

In this paper, the physical layer security based on the ergodic secrecy rate (ESR) of SM system is investigated. We consider imperfect channel information (CSI) and evaluate the secrecy performance over Rayleigh channels. The ergodic rate and its lower bound for the legitimate receiver and eavesdropper are, respectively, derived. On the basis of these derivations, we further derive the system ESR, and obtain two approximated expressions as provided in equations (23) and (24). The former requires mean computation, and the latter can provide closed-form expression. Theoretical expressions for a special case of perfect CSI are also derived, as given in equations (25) and (26). With these theoretical expressions, the secrecy performance of the SM system with artificial noise and imperfect CSI is effectively evaluated, and the impact of estimation error and artificial noise on the system performance is analyzed well. Results show that the ESR exhibits obvious degradation when the estimation error variance is beyond 0.01. Also, after an initial increase, the ESR decreases eventually, with increasing power of the artificial noise. Simulation results comply with the theoretical analysis thereby validating the derived mathematical expressions. Namely, the theoretical ESR curve is in close agreement with the corresponding simulation curve, and the system ESR under imperfect CSI is lower than that under perfect CSI, as expected.

## ACKNOWLEDGMENT

The authors would like to thank the anonymous reviewers for their valuable comments which improve the quality of this paper.

## REFERENCES

- [1] P. Yang, M. Di Renzo, Y. Xiao, S. Li, and L. Hanzo, "Design guidelines for spatial modulation," *IEEE Commun. Surveys Tuts.*, vol. 17, no. 1, pp. 6–26, 1st Quart., 2015.
- [2] R. Y. Mesleh, H. Haas, S. Sinanovic, C. W. Ahn, and S. Yun, "Spatial modulation," *IEEE Trans. Veh. Technol.*, vol. 57, no. 4, pp. 2228–2241, Jul. 2008.
- [3] X. Wang, X. Wang, and L. Sun, "Spatial modulation aided physical layer security enhancement for fading wiretap channels," in *Proc. IEEE Int. Conf. Wireless Commun. Signal Process. (WCSP)*, Yangzhou, China, Oct. 2016, pp. 1–5.
- [4] Y.-S. Shiu, S. Y. Chang, H.-C. Wu, S. C.-H. Huang, and H.-H. Chen, "Physical layer security in wireless networks: A tutorial," *IEEE Wireless Commun.*, vol. 18, no. 2, pp. 66–74, Apr. 2011.
- [5] F. Shu, L. Xu, J. Wang, W. Zhu, and X. Zhou, "Artificial-noise-aided secure multicast precoding for directional modulation systems," *IEEE Trans. Veh. Technol.*, vol. 67, no. 7, pp. 6658–6662, Jul. 2018, doi: 10.1109/TVT.2018.2799640.
- [6] H.-M. Wang, C. Wang, D. W. K. Ng, M. H. Lee, and J. Xiao, "Artificial noise assisted secure transmission for distributed antenna systems," *IEEE Trans. Signal Process.*, vol. 64, no. 15, pp. 4050–4064, Aug. 2016.
- [7] C. Wang and H.-M. Wang, "Robust joint beamforming and jamming for secure AF networks: Low complexity design," *IEEE Trans. Veh. Technol.*, vol. 64, no. 5, pp. 2192–2198, May 2015.
- [8] H.-M. Wang, C. Wang, and D. W. K. Ng, "Artificial noise assisted secure transmission under training and feedback," *IEEE Trans. Signal Process.*, vol. 63, no. 23, pp. 6285–6298, Dec. 2015.
- [9] F. Shu et al., "Low-complexity and high-resolution DOA estimation for hybrid analog and digital massive MIMO receive array," *IEEE Trans. Commun.*, vol. 66, no. 6, pp. 2487–2501, Jun. 2018.
- [10] F. Shu et al., "Secure and precise wireless transmission for random-subcarrier-selection-based directional modulation transmit antenna array," *IEEE J. Sel. Areas Commun.*, vol. 36, no. 4, pp. 890–904, Apr. 2018, doi: 10.1109/JSAC.2018.2824231.
- [11] X. Guan, Y. Cai, and W. Yang, "On the secrecy mutual information of spatial modulation with finite alphabet," in *Proc. IEEE Int. Conf. Wireless Commun. Signal Process. (WCSP)*, Huangshan, China, Oct. 2012, pp. 1–4.
- [12] L. Wang, S. Bashar, Y. Wei, and R. Li, "Secrecy enhancement analysis against unknown eavesdropping in spatial modulation," *IEEE Commun. Lett.*, vol. 19, no. 8, pp. 1351–1354, Aug. 2015.
- [13] Z. Gao, H. Hu, D. Cheng, J. Xu, and X. Sun, "Physical layer security based on artificial noise and spatial modulation," in *Proc. IEEE Int. Conf. Wireless Commun. Signal Process. (WCSP)*, Yangzhou, China, Oct. 2016, pp. 1–5.
- [14] C. Liu, L.-L. Yang, and W. Wang, "Secure spatial modulation with a full-duplex receiver," *IEEE Wireless Commun. Lett.*, vol. 6, no. 6, pp. 838–841, Dec. 2017.
- [15] J. Jeganathan, A. Ghayeb, and L. Szczecinski, "Spatial modulation: Optimal detection and performance analysis," *IEEE Commun. Lett.*, vol. 12, no. 8, pp. 545–547, Aug. 2008.
- [16] A. Hyadi, Z. Rezki, A. Khisti, and M. S. Alouini, "Secure broadcasting with imperfect channel state information at the transmitter," *IEEE Trans. Wireless Commun.*, vol. 15, no. 3, pp. 2215–2230, Mar. 2016.
- [17] X. Zhou and M. R. McKay, "Secure transmission with artificial noise over fading channels: Achievable rate and optimal power allocation," *IEEE Trans. Veh. Technol.*, vol. 59, no. 8, pp. 3831–3842, Oct. 2010.
- [18] J. Hu, S. Yan, F. Shu, J. Wang, J. Li, and Y. Zhang, "Artificial-noise-aided secure transmission with directional modulation based on random frequency diverse arrays," *IEEE Access*, vol. 5, pp. 1658–1667, 2017.
- [19] S. Yun, S. Im, I.-M. Kim, and J. Ha, "On the secrecy rate and optimal power allocation for artificial noise assisted MIMOME channels," *IEEE Trans. Veh. Technol.*, vol. 67, no. 4, pp. 3098–3113, Apr. 2018.
- [20] I. S. Gradshteyn and I. M. Ryzhik, *Table of Integrals, Series, and Products*, A. Jeffrey and D. Zwillinger, Eds., 7th ed. Salt Lake City, UT, USA: Academic, 2007, p. 347.



**XIANGBIN YU** received the Ph.D. degree in communication and information systems from the National Mobile Communications Research Laboratory, Southeast University, China, in 2004. From 2010 to 2011, he was a Research Fellow with the Department of Electronic Engineering, City University of Hong Kong. From 2014 to 2015, he was a Visiting Scholar with the Department of Electrical and Computer Engineering, University of Delaware, USA. He is currently a Full Professor with the Nanjing University of Aeronautics and Astronautics, China. His research interests include distributed MIMO, adaptive modulation, pre-coding design, and green communication. He has served as a Technical Program Committee Member of the 2006 and 2017 IEEE Global Telecommunications Conferences, the 2011 and 2017 Wireless Communications and Signal Processing, and the 2015 and 2018 IEEE International Conference on Communications. He has been a member of the IEEE ComSoc Radio Communications Committee since 2007, and a Senior Member of the Chinese Institute of Electronics since 2012. He is also a reviewer for several journals.



**YAPING HU** received the B.Sc. degree from the Nanjing University of Aeronautics and Astronautics, Nanjing, China, in 2017, where he is currently pursuing the M.Sc. degree.



**QING PAN** received the B.Sc. degree from the Nanjing University of Aeronautics and Astronautics, Nanjing, China, in 2016, where she is currently pursuing the M.Sc. degree.



**XIAOYU DANG** received the Ph.D. degree in electrical engineering from Brigham Young University, Provo, UT, USA, in 2009. From 2016 to 2017, he was a Visiting Scholar with The University of Tennessee, USA. He is currently a Full Professor with the College of Electronics and Information Engineering, Nanjing University of Aeronautics and Astronautics, Jiangsu, China. His technical interests include coding and modulation, diversity techniques, and reliable transmission of signals in deep space environments.



**NING LI** received the M.Phil. degree in manufacturing engineering and engineering management from the City University of Hong Kong, in 1999. She is currently an Associate Professor with the Department of Information and Communication Engineering, College of Electronic and Information Engineering, Nanjing University of Aeronautics and Astronautics. Her research interests include digital image processing, computer vision, and object detection and tracking.



**MAQSOOD HUSSAIN SHAN** is currently pursuing the Ph.D. degree with the Nanjing University of Aeronautics and Astronautics.

• • •